The Synthesis of Activated Carbon from Waste Tyre as Fuel Cell Catalyst Support

Taufany, Fadlilatul
Department of Chemical Engineering, Institut Teknologi Sepuluh Nopember

Mathilda Jowito Pasaribu
Department of Chemical Engineering, Institut Teknologi Sepuluh Nopember

Berlina Yunita Sari Romaji
Department of Chemical Engineering, Institut Teknologi Sepuluh Nopember

Rahmawati, Yeni
Department of Chemical Engineering, Institut Teknologi Sepuluh Nopember

他

https://doi.org/10.5109/4794166

出版情報：Evergreen. 9 (2), pp.412-420, 2022-06. 九州大学グリーンテクノロジー研究教育センター
バージョン：

The Synthesis of Activated Carbon from Waste Tyre as Fuel Cell Catalyst Support

Fadlilatul Taufany[1*], Mathilda Jowito Pasaribu[1], Berlina Yunita Sari Romaji[1], Yeni Rahmawati[1], Ali Altway[1], Susianto[1], Siti Nurkhamidah[1], Julfikar Gilang Anfias[1], Yuliani Mursidah[1], Desi Fujanita[1], Susan Yulianti[1], Dian Rahmawati[1], Ghea Stellarosari[1]

[1]Department of Chemical Engineering, Institut Teknologi Sepuluh Nopember

*Author to whom correspondence should be addressed:
E-mail: f_taufany@chem-eng.its.ac.id

(Received December 7, 2021; Revised May 31, 2022; accepted May 31, 2022).

Abstract: This study synthesized the activated carbon as material support for platinum catalysts in fuel cells application. The pyrolytic carbon black from the waste tyre was activated through physical activation using oxygen gas in a vertical bed column. The activation influencing factors are then examined, which include the activation temperature, the activation time, and the composition of oxidant oxygen gas in the activation. The results showed that the optimum operating conditions for the carbon black activation into its corresponding activated carbon are activation temperature at 300°C, activation time for 1 hour with pure oxidant oxygen gas. The resulting activated carbon was also successfully tested as a potential platinum-fuel cell catalyst support (Pt/AC) in the methanol oxidation reaction (MOR) in Direct Methanol Fuel Cell (DMFC) application, as indicated from the electrochemical testing, *i.e.* the cyclic voltammetry (CV) and linear sweep voltammetry (LSV) measurement. The CV measurement showed that this Pt/AC catalyst generates the region of hydrogen adsorption/desorption ($H_{ads/des}$), the double-layer charging and discharging, and the CO oxidation-reduction. In addition, during the LSV measurement, this Pt/AC catalyst showed the reactivity towards MOR with its current density of 0.0005 $A.cm^{-2}$ at 0.6 V.

Keywords: activated carbon; carbon black; physical activation; Direct Methanol Fuel cell

1. Introduction

The electrochemical reaction of converting chemical power into electrical power in a fuel cell (FCs) has become an encouraging option for power generation technology which is receiving increasing attention around the world[1,2]. It generates low-cost production but discovers stable materials and achieves an excellent fuel cell system performance. The disadvantages of fuel cell technology are high intrinsic costs in the system and poor durability[2].

Specific ranges of fuel cell materials science have gotten further consideration to develop inexpensive and durable materials. On Pt catalyst development, enhancement on use and activity has resulted in remarkable reductions in Pt loading; however rising Pt costs threaten to weaken this advance. Currently, carbon materials are widely utilized to support Pt nanoparticles for practical and inexpensive purposes[3]. A new interest has been raised on the carbon-supported bimetallic system of its suitability as the catalyst in direct methanol fuel cells (DMFCs) for the methanol oxidation[4]. The special character of carbon materials, including being good conductivity, relatively stable in both acidic and basic electrolytes, and equipping large surface area for metal catalyst dispersion are the reasons why carbon materials are widely utilized as catalyst supports[5].

Recently there has been advanced research to develop carbon supports with a different morphology from carbon materials, which have high mechanical strength and stability, outstanding biocompatibility[6], good electron conductivity, and high surface area, such as carbon nanofibers[7,8,9,10], carbon nanotubes[11,12], airgel carbon[13,14] and ordered mesoporous carbon (ordered mesoporous carbon)[15,16,17]. However, it should be noted that the process of synthesizing carbons with unique morphology is very complex and expensive, which requires advanced technology such as arc discharge, chemical vapor deposition, laser ablation, electrospinning, and high-pressure carbon monoxide disproportionation.

Carbon materials, such as carbon black, are often employed as catalytic support for Pt catalysts in fuel cells [18]. However, in order to achieve high metal dispersion and increased catalytic activity within the fuel cell, the material support is expected to have a large surface area

[19]. Carbon black with a low surface area - around 60-80m^2/g[20] - needs to activate to obtain a higher surface area and capability to adsorb molecules[21]. The activated carbon for fuel cell support material can be synthesized by pyrolysis of waste tires to form carbon black. Pyrolysis is the thermochemical conversion process without involving oxygen[22] to produce a bio-oil, charcoal, and syngas[23]. Waste management, namely the disposal of waste tyres, is currently a serious concern over the world. An estimated 1.2 billion tons of waste rubber are produced each year worldwide, with 11% of waste tires being exported, 27% being illegally dumped or thrown away, and only 4% being used in civil engineering projects. As a result, attempts were conducted to identify the potential for waste tires to be used in civil engineering projects[24].

Previously mentioned work focused on research of synthesis activated carbon from pyrolytic carbon black with physical activation using oxygen as an oxidant. Some gases that are commonly used as oxidant in activation of carbon are CO_2, N_2, air, or steam[25]. Compared to other oxidant gas, such as CO_2[26] and steam[27], oxygen provides lower temperature and shorter time in the carbon activation process which will be proven within this study. We will include the discussion of the effect of activation temperature, carbon activation time, oxygen composition used as oxidants, and proximate analysis of pyrolytic carbon black and mesoporous carbon after gas treatment. In addition, it is also explained about activated carbon from carbon black pyrolytic as fuel cell catalyst support.

2. Materials and Methods

2.1.Materials

The raw carbon black was obtained from the pyrolysis of waste tyre. Oxygen gas with purity of 99.6 – 99.8% (PT. Samator), nitrogen gas with purity of minimum 99.999% (PT. Samator), millipore water (18 MW), ethylene glycol (Across), platinum precursor salts ($H_2PtCl_6 \cdot 6H_2O$, Alfa Aesar), and sulfuric acid (Acros) were utilized.

2.2.Methodology

2.2.1. Pyrolysis of Waste Tyre

The method of pyrolysis of waste tyre was described in our previous report[28]. The raw material, *i.e*. waste tyre, was obtained from retreated seller. The waste tyre was washed with water and steel wires were removed. The cleaned tyre was dried under sunlight for hours and milled and continued with screening to obtain particles size of -20/+30 mesh, which was similar to around 0.687 mm[28] The 30 g of this cleaned tyre was then put inside thesample place, and it was introduced into the semi-batch reactor whose temperature and heating rate could be controlled and be conducted at 900 °C. The reactor was closed tightly, and nitrogen has flowed to the reactor with a rate of 1000 mL/minute for ± 40 minutes purposing eliminating oxygen and impurities from the air. The rate of nitrogen gas was controlled by the gas flow meter. The reactor was heated by an electrical heater starting at room temperature until 600 °C, controlled by a PID instrument by reading the electrical pulses transmitted from the thermocouple inside the reactor. Pyrolysis took time for 90 minutes, and the heating rate was set at 10 °C/minute. The pyrolysis time was recorded when the temperature was attained and then maintained until determined duration as described previously. Nitrogen gas has flowed continually into the reactor during pyrolysis. A condenser was connected to the reactor functioning to change the gas to the liquid phase of the pyrolytic product. The gas produced from the heating of particles passed through a condenser and cooled until 30 °C. The condensed product was kept inside liquid storage, while the vapor that was not changed into liquid, was channeled to gas storage. The pyrolysis process was conducted at atmospheric pressure. The sample (solid) was removed from the reactor after pyrolysis was completely finished.

2.2.2. Activation of Pyrolytic Carbon Black

During the pyrolysis process, the waste tyre was converted into the carbon residue. It contains enough carbon char residue which can be converted into the activated carbon. A total of 5 grams of pyrolysis carbon black with a size of 120 mesh was inserted into a vertical column with temperatures 300°C and 450°C. Then oxidant gas used was oxygen with a 100 mL/minute flow rate for 1 and 2 hours and variable composition of 10%, 20%, and 100%. The final stage is TPD characterization test using Micromeritics-AutoChem II, Chemisorption Analyzer, TGA analysis using TGA/DSC 1 GC 200, mass loss analysis, and iodine number analysis using Titrimetry method.

2.2.3. Synthesis of Carbon Supported Pt Catalyst (Pt/AC)

The method of synthesis of Pt/AC was described inour previous report[22]. First step, as much as 1.2 mmol of $H_2PtCl_6.6H_2O$ solution in 10 mL ethylene glycol was stirred at a constant speed for 10 min at ambient temperature. Next, glycolic acid as much as 1.6 mmol was added to this solution and stirred at a constant speed for 30 min. After that, 0.640 g AC was added, and the resulting solution was placed in an ultrasonic bath for around 30 min. The pH of the EG solution was adjusted to 11 by adding a dropwise saturated NaOH to it. The resulting mixture was set in a microwave reactor at 808°C at 300 Watt power for around 1 hour and washed using a centrifugal pump that has a high-power of 22000 rpm for 30 min. The nanoparticles were washed and rediffused using cyclohexane and ethanol. To remove organic remains from the mixture, this method was repeated five times. After removing the residues, the sample was dried for around 8 h in an air oven at 80°C. To achieve complete elimination of all organic residual components, the nanoparticles were treated at 300 °C for 2 h with a 10% H_2 gas.

2.2.4. Electrode Preparation and Electrochemical Measurement

The electrode preparation method andelectrochemical measurement were described in our previous report[29]. Experiments have been performed at ambient temperature (25±1) °C. A three-electrode electrochemical cell was used in the electrochemical studies. A Pt counter electrode and a reference saturated calomel electrode (SCE) (all potentials in this experimentwere compared to a reversible hydrogen electrode (RHE). The Solartron potentiometer/galvanostat (model 1480) instrument was utilized in these electrochemicalmeasurements. A Pt/AC catalyst was mounted on the surface area (0.1964 cm^2) of a free carbon electrode (GCE) to serve as the working electrode. The procedure of electrode's preparation consisted of first, a specified amount of Pt / AC powder is dispersed in 0.5% Nafion, and then sonicating it to obtain clear suspension; Second, place an aliquot of the suspension on a GCE disc, equal to7 µL of 6.2 μg_{Pt}/mL catalysts. Third, a uniform catalyst membrane was obtained by sequential air drying at ambient temperature for about 5 min and air drying at 80°C. All studies used 0.5 M sulfuric acid as the supporting electrolyte. Prior to the electrochemical experiment, the electrodes were immersed in N_2-saturatedsulfuric acid (200 mL, 0.5 M) and the potential wasscanned from 0.00 to 1.1 V (RVE) for 10 cycles at 0.05 Vs^{-1}. Then, using a scan rate of 10 mVs^{-1}, we performed cyclic voltammetry tests. MOR electrochemical measurements were carried out using a combination of linear sweep voltammetry (LSV) and a rotating disk electrode (RDE) equipment (Autolab speed control), in a mixture of 0.5 M H_2SO_4 and 10 vol% CH_3OH, at a scan rate of 1 mVs^{-1}in the potential range of 0.05 to 1.0 V.

3. Results and Discussion

The activation of carbon black using a vertical bed column aims to synthesize activated carbon so that it has a high specific surface area of >800 m^2/g[30]. The activation process for carbon black uses a variable activation temperature below the onset temperature/maximum temperature of its decomposition, to gently decompose the carbon in such a way that carbon black can form a new morphology mesoporous carbon, *i.e*. activated carbon. The onset temperature/maximum temperature of decomposition is the temperature at which a material will begin to lose a large amount of mass. This temperature was obtained from the temperature programmed desorption (TPD) and the thermogravimetric analysis (TGA) analysis, where the results of the TPD analysis (Supporting Information **Figure S1**) showed that carbon black began to decompose at the onset temperature of 600°C. Meanwhile, the results of the TGA analysis (Supporting Information **Figure S2**) showed that carbon black began to decompose at its onset temperature of 630°C. These results determined the activation temperature variables below than the onset temperature/maximum temperature of its decomposition, *i.e.* at 300°C and 450°C, using a vertical gas treatment column with a contact activation time of oxidant gas (O_2) for 1-2 hours.

3.1.Influence of Activation Temperature

Four samples of pyrolytic carbon black were prepared to study the influence of the activation temperature and activation time on their corresponding mass loss and iodine number, as described as follows:

a) Sample S-1h-300C: The sample is subjected into O_2 gas with a flow rate of 100 mL/minute for 1 hour at the temperature of 300°C.
b) Sample S-2h-300C: The sample is subjected into O_2 gas with a flow rate of 100 mL/minute for 2 hours at the temperature of 300°C.
c) Sample S-1h-450C: The sample is subjected into O_2 gas with a flow rate of 100 mL/minute for 1 hour at the temperature of 450°C.
d) Sample S-2h-450C: The sample is subjected into O_2 gas with a flow rate of 100 mL/minute for 2 hour at the temperature of 300°C.

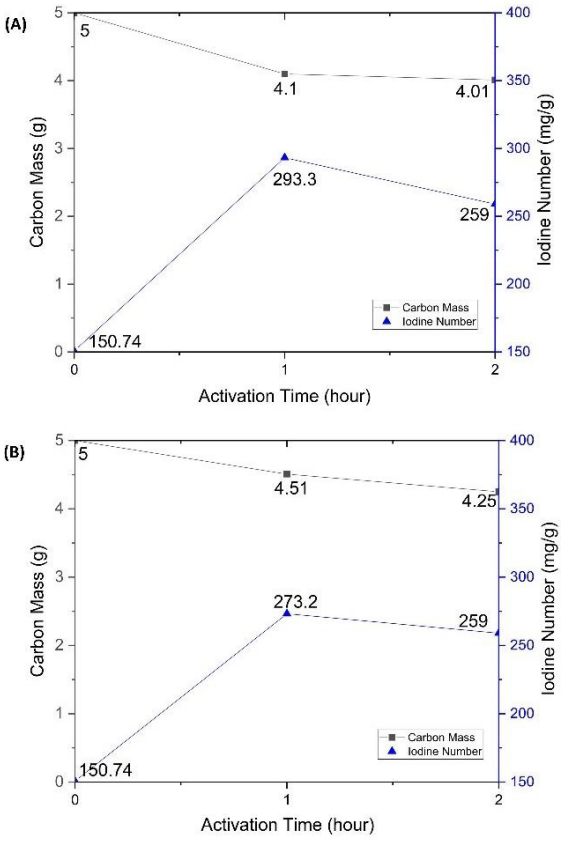

Fig. 1: Mass loss and iodine number of the activated carbon after subjected into O_2 gas with a flow rate of 100 mL/minute for 2 hours activation time in a vertical gas column at a temperature of (A) 300°C and (B) 450°C.

As can be seen from **Figure 1**, the decrease of carbon mass that is activated at 450°C were slower than the one activated at 300°C. For the activation temperature of 300°C, the carbon tends to lose its mass from 5 grams to

4.1 grams, and then to 4.01 grams, for the activation time of 1 and 2 hours, respectively. Meanwhile for the activation temperature of 450°C, the carbon tends to lose its mass from 5 grams to 4.51 grams, and then to 4.25 grams, for the activation time of 1 and 2 hours, respectively. Interestingly, this has an impact on the resulting iodine number of the carbon, where the iodine number of the carbon after 1 hour activation temperature at 450°C (*i.e*. 273.2 mg/g) was smaller than that of 300°C (*i.e*. 293.3 mg/g).

When the activation temperature is increased, the iodine number decreases until it reaches its maximum value. The incident was probably in connection to the fact that when burn-off increases, the overall volume of macropores diminishes. Weight loss became determined now no longer to result in the formation of new micropores, but the higher amount of carbon burnt, and unstable compounds released as the activation rate got faster due to higher activation temperature[31]. Thedecrease in the absolute micropore volume of micropores more burn-off may hinder the burning of the walls between adjacent pores. As a result of this activity, the micropores expand into bigger pores[32]. The higher the activation temperature will degrade more organic molecules into tar and light gases, which was indicated bythe decrease of mass carbon[25].

3.2.Influence of Activation Time

Figure 1 shows that for 2 hours activation time, the highest iodine number is obtained at the first 1 hour activation and then decreases for the next 1 hour. For activation at a temperature of 300°C in a vertical gas column, the iodine number increased from 150.74 mg/g to 293.3 mg/g as the activation time increased from initial condition until 1 hour. The iodine number then decreased from 293.3 mg/g to 259 mg/g as the activation time increased to 2 hours. This suggests that activation has a maximum time and can be disadvantageous if the activation exceeds the maximum activation time. The carbon pores will enlarge during the activation below the maximum activation time and will be damaged if it takes a longer time[33]. The longer the activation time, the more carbon mass will be decreased. This mass loss is an indication of damaged pores[32].

The present finding is also in a good agreement with study reported by Nayak et al[34], where the optimum activation time was obtained up to 1 hour, due to enlargement of the carbon micropores that can also cause the increase of its carbon surface area. After 1 hour activation time, they also observed the decrease in carbon surface area and subsequently carbon micropores. The yield of activated carbon decreases due to carbon burn-off by increasing activation time[35]. In a detailed inspection in **Figure 1**, particularly up to 1 hour for the optimum activation time, both carbon black samples after treated at temperature of 300°C and 450°C exhibiting a similar trend, where the higher carbon weight loss tends to boost the formation of carbon micropores, resulting in an increased surface area and subsequent increased iodine number, in accordance with the findings reported by Sahin et.al.[33]

3.3.Influence of Oxygen Composition

Figure 2 shows that the higher composition of oxygen, the higher the iodine number of carbon. The highest iodine number attained at 259 mg/g with an oxygen composition of 100%. A similar result was also reported by Omer Sahin[33] that increment of iodine number was because of the development of pores and carbon porosity as composition of oxidizing agent increased.

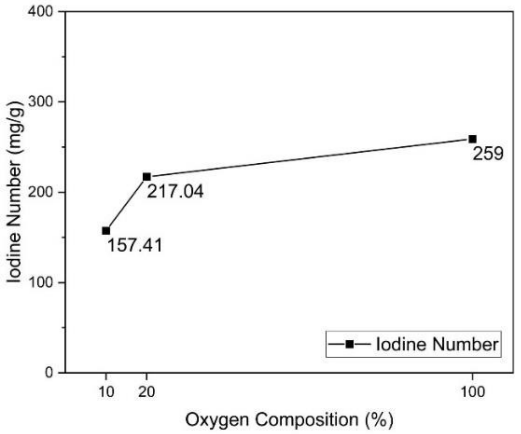

Fig. 2: The influence of oxygen composition (10%, 20%, and 100%) on the iodine number of carbon with an activation temperatureof 300°C for 2 hours in a vertical gas column.

The composition of 20 % O_2 gas purity was designed to mimic the composition of the O_2 in the air. Moreover, the resulting iodine numbers of the activated carbon after treated with 20 % and 100 % O_2 gas purity were found not to be significance difference, *i.e.* 217.04 mg/g and 259 mg/g, respectively. Consequently, these findings lead to the optimum operating condition for activating the carbon black, which is O_2 gas purity of 20% at a flowrate of 100 ml/minute, and a temperature of 300°C for 1 hour. The resulting activated carbon was then subjected into a proximate analysis with the aims to determine its moisture, volatile matter, fix carbon, and ash content[36].

During the activation, there is a release of volatile substances that increase the carbon content[37]. **Table 1** shows that the volatile matter carbon from pyrolysis to activated carbon decreased from 13.84% to 9.02% and the moisture content also decreased from 3.57% to 1.37%. Reducing the percentage of this component increases the percentage of fixed carbon from 67.73% to 80.22%. This is because the carbon activation process can cause unstable organic molecules. The bonds betweenmolecules are broken and make volatile matter in the material lose into gas and liquid products so that the carbon fix is higher[38]. The residue left after all combustible matter in the activated carbon has been entirely burned away is referred to as ash content, and it reflects the quality of

mineral matter in the liquid under test[39]. The ash content of carbon after activation with O_2 oxidant gas decreased from 14.86% to 9.02%. The ash content influences the AC adsorption capacity since it is related to AC pore structure. The adsorption capacity of the AC generated increases as the ash concentration lowers[40]. Because the pores of activated carbon are filledwith metallic elements such as magnesium, calcium, and potassium, ash content might impair the adsorption capacity of the material[41].

Table 1. The characterization of pyrolytic carbon black and its corresponding activated carbon after subjected into 20% O_2 gas with a flowrate of 100 mL/minute, at a temperature of 300°C for 1 hour

No.	Characterization	Pyrolytic Carbon Black	Activated Carbon
1	Iodine Number	150.74 mg/g	572 mg/g
2	Fixed Carbon	67.73%	80.22%
3	Volatile Matter	13.84%	9.02%
4	Moisture Content	3.57%	1.37%
5	Ash Content	14.86%	9.02%

3.4.Electrocatalytic activities in Methanol Oxidation Reaction

Electrochemical studies were conducted by using CV and LSV, to investigate the ability of the resulting activated carbon as a Pt fuel cell catalyst support, where the results were presented in **Figures 3** and **Figure 4**, respectively. The carbon-supported Pt (Pt/AC) catalyst in this study uses a metal Pt-loading of 20 wt%. Generally, the unsupported or carbon-supported Pt is utilized as the catalyst in PEMFC and DMFC over other monometallic catalysts because of the following reasons: (a) The anodic and cathodic reactions have a high exchange current density, (b) the adequate slope of Tafel at all the potentials, and (c) the capacity to oxidize the fuel (*i.e.* methanol), particularly on the anode side of fuel cells.

In region 1, the desorption of the adsorbed hydrogen, *i.e*. H-ads, from the surface of Pt catalyst is depicted, with potentials varying from 0.06 to 0.32 V vs. RHE. The hydrogen desorption with the unified anodic charge below the hydrogen desorption area ($Q_{H\text{-}des}$, in Coulombs) revealed multiple well-defined peak pairs because of the existence of distinct Pt crystalline facets. At the region 2, which extending from the potential of 0.32 to 0.68 V vs. RHE shows the double layer phenomenon of charging and discharging. Two peaks can be observed in the anodic area, that is at the potential higher than 0.68 Vvs. RHE, labelled as regions of 3 and 4. The production ofOH and O on the Pt catalyst surface are seen in regions 3 and 4, respectively. Pt catalyzes the dissociation of water, resulting in an oxide layer on the Pt surface.

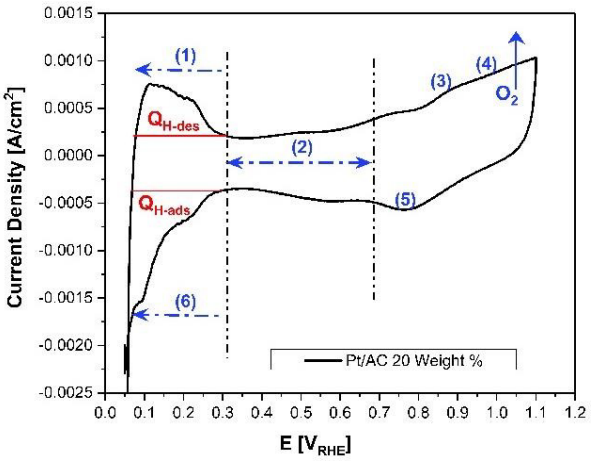

Fig. 3: Cyclic voltammetry on Pt/AC catalyst performed in thenitrogen-saturated 0.5 M sulfuric acid solution, recorded at the scan rate of 10 mVs^{-1} andambient temperature of 25°C

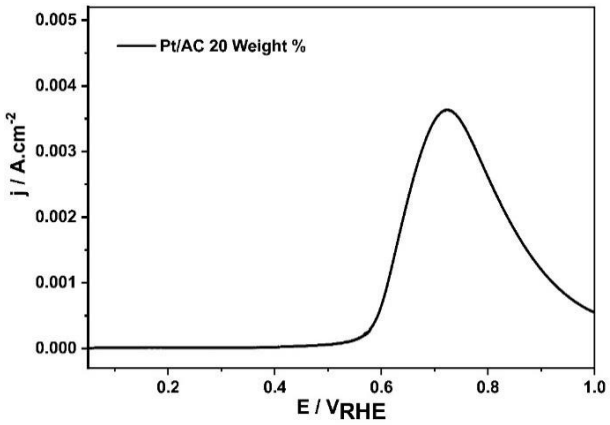

Fig. 4: Linear scan voltammogram for the MOR on Pt/AC catalyst performed in the nitrogen-saturated 0.5 M sulfuric acid solution with the addition of 5 vol% methanol (20 mL), recorded at 1 mV s^{-1} and 25°C with a rotation rate of 1600 rpm

After region 4, the oxygen gas evolution takes over, necessitating an instantaneous reverse scan. The reduction of the oxide layer can be seen when the scanning direction is reversed(Region 5). When compared to the peak of oxide creation,the peak of oxide reduction was observed at the lower potentials, that is below than the potential of 0.32 V vs. RHE. In this region, proton reduction causes underpotential deposition of hydrogen atoms shown on cathodic scan. $Q_{H\text{-}ads}$ (in Coulombs) stands for the integrated cathodic charge of hydrogen adsorption. The hydrogen adsorption to the hydrogen desorption observation. For distinct Pt crystalline facets, the ratio of $Q_{H\text{-}des}/Q_{H\text{-}ads}$ can yield a several pairs of clear-defined peaks, which is similar information on the reversibility reaction of hydrogen adsorption/desorption, which is denoted as H-ads/H-des. It is essential to note that the Pt-catalyst roughness factor, and the electrochemical active surface area can all be determined by using the electrochemical CV measurement[42].

The LSV measurement was carried out to evaluate the

kinetic properties of Pt /AC catalyst towards MOR[43]. It is generally known that in LSV for the MOR, the lower the onset potential, the higher the associated catalytic activity. As can be seen in the **Figure 4**, the current density of Pt/AC catalyst with Pt-catalyst weight loading of 20%, at 0.6 V was found to be 0.0005 A.cm^{-2}, indicating that the resulting of Pt/AC catalyst is active for MOR in DMFC. Moreover, a distinctive adsorbed layer's oxidative stripping peak in MOR was also clearly observed at 0.58~1.0 V. This oxidative stripping peak, which has been observed during the MOR process, indicating that the methanol is sequentially adsorbed, dissociated, and then dehydrogenated on Pt active sites to produce an intermediate [41].

4. Conclusion

The synthesis of the activated carbon as fuel cell catalyst support was strongly influenced by the activation temperature, the activation time, and the oxygen composition as the oxidizing agent. Based on the carbon mass loss and iodine number analysis, the highest iodine number was found to 293.3 mg/g at the activation temperature of 300 ℃ and 1 hour activation time. The higher concentration of oxygen as an oxidizing agent resulted in a higher iodine number. However, the use of 20 % O_2 gas purity was favorable, as it mimics the composition of O_2 in air, and the resulted iodine number (*i.e*. 217.04 mg/g) was found not to be significance difference with that of 100% O_2 gas purity, *i.e.* 259 mg/g. The resulting activated carbon has been found to be successfully served as a fuel cell catalyst, as can be observed from the electrochemical measurements of CV and LSV. The CV measurement clearly showed the presence of Pt/AC catalyst behaviors on the adsorption-desorption process of hydrogen, the double layer of charging and discharging, and the hydrogen adsorption-desorption process, on the surface of Pt/AC catalyst. The oxidation process occurred at the region 3-4, while the reduction of oxide layer occurred at region 5. The desorption process of adsorbed hydrogen on the surface of Pt catalyst occurred in region 6. Whereas based on the linear sweep voltammetry measurement result, the current density of Pt/AC catalysts at 0.6 V is 0.0005 A.cm^{-2}.

Acknowledgements

The authors gratefully acknowledge the financial support from the the Institut Teknologi Sepuluh Nopember for this work, under project scheme of the PPHKI 2021.

Supporting Information

Results showing TPD profile for the resulted pyrolytic carbon black (**Figure S1**), and mass loss profile of the resulted pyrolytic carbon black containing sample during TGA (**Figure S2**) are available free of charge via the internet at EVERGREEN Joint Journal of Novel Carbon Resource Sciences & Green Asia Strategy.

References

1) Karim NA, Kamarudin SK, Shyuan LK, Yaakob Z, Daud WRW, Kadhum AAH, "Study on the electronic properties and molecule adsorption of W18O49 nanowires as a catalyst support in the cathodes of direct methanol fuel cells," *J Power Sources* **288**, 461–472 (2015). doi: 10.1016/j.jpowsour.2015.04.111.
2) Sharma S, Pollet BG, "Support materials for PEMFC and DMFC electrocatalysts—a review," *J Power Sources* **208**, 96–119 (2012).doi:10.1016/j.jpowsour.2012.02.011.
3) Holdcroft, S., "Fuel cell catalyst layers: a polymer science perspective," *Chemistry of materials*, **26**(1), 381-393 (2014).doi: 10.1021/cm401445h.
4) Vecchio, C. L., Sebastián, D., Alegre, C., Aricò, A. S.,& Baglio, V., "Carbon-supported Pd and Pd-Co cathode catalysts for direct methanol fuel cells (DMFCs) operating with high methanol concentration," *Journal of Electroanalytical Chemistry*, **808**, 464-473 (2018).doi:10.1016/j.jelechem.2017.02.042.
5) Ramli, Z.A.C. and Kamarudin, S.K., "Platinum-based catalysts on various carbon supports and conducting polymers for direct methanol fuel cell applications: a review," *Nanoscale research letters*, **13**(1), 1- 25(2018).doi: 10.1186/s11671-018-2799-4.
6) Talib, N., Jamaluddin, N.A., Sheng, T.K., Kiow, L.W., Abdullah, H., Ahmad, S. and Saleh, A., "Tribological Study of Activated Carbon Nanoparticle in Nonedible Nanofluid for Machining Application," *Evergreen: joint journal of Novel Carbon Resource Sciences & Green Asia Strategy* **8**, Issue 02, 454-460 (2021). doi:10.5109/4480728.
7) Gangeri, M.; Centi, G.; Malfa, A. L.; Perathoner, S.; Vieira, R.; Pham-Huu, C.; Ledoux, M. J., "Electrocatalytic performances of nanostructured platinum-carbon materials," *Catalysis Today,***50** , 102–103, (2005).doi: 10.1016/j.cattod.2005.02.035.
8) Ismagilov, Z. R.; Kerzhentsev, M. A.; Shikina, N. V.; Lisitsyn, A. S.; Okhlopkova, L. B.; Barnakov, C. N.; Sakashita, M.; Iijima, T.; Tadokoro, K, "Development of active catalysts for low Pt loading cathodes of PEMFC by surface tailoring of nanocarbon materials," *Catalysis Today*, **58**,102–103, (2005).doi: 10.1016/j.cattod.2005.02.007.
9) Yuan, F.; Yu, H. K.; Ryu, H., "Preparation and characterization of carbon nanofibers as catalyst support material for PEMFC," *Electrochimica Acta*, **50**, 685 (2004).doi: 10.1016/j.electacta.2004.01.106.
10) Zhang, L.; Cheng, B.; Samulski, E. T., "In situ fabrication of dispersed, crystalline platinum nanoparticles embedded in carbon nanofibers," *Chemical Physics Letters*, **398**, 505 (2004).doi: 10.1016/j.cplett.2004.09.120.
11) de Paula, C. C.; Garcia Ramos, A.; da Silva, A. C.;

Cocchieri Botelho, E.; Rezende, M. C., "Fabrication of glassy carbon spools for utilization in fiber optic gyroscopes," *Carbon*, **40**, 787 (2002).doi: 10.1016/s0008-6223(01)00136-1.

12) Tang, H.; Chen, J. H.; Huang, Z. P.; Wang, D. Z.; Ren, Z. F.; Nie, L. H.; Kuang, Y. F.; Yao, S. Z., "High dispersion and electrocatalytic properties of platinum on well-aligned carbon nanotube arrays," *Carbon*, **42**, 191 (2004).doi: 10.1016/j.carbon.2003.10.023.
13) Marie, J.; Berthon-Fabry, S.; Achard, P.; Chatenet, M.; Pradourat, A.; Chainet, E., "Highly dispersed platinum on carbon aerogels as supported catalysts for PEM fuel cell-electrodes: comparison of two different synthesis paths," *Journal of Non-Crystalline Solids*, **350**, 88 (2004).doi: 10.1016/j.jnoncrysol.2004.06.038.
14) Smirnova, A.; Dong, X.; Hara, H.; Vasiliev, A.; Sammes, N., "Novel carbon aerogel-supported catalysts for PEM fuel cell application," *International Journal of Hydrogen Energy*, **30**, 149 (2005).doi: 10.1016/j.ijhydene.2004.04.014.
15) Joo, J. B.; Kim, P.; Kim, W.; Kim, J.; Yi, J., "Preparation of mesoporous carbon templated by silicaparticles for use as a catalyst support in polymer electrolyte membrane fuel cells,"*Catalysis Today*, **111**, 171 (2006).doi: 10.1016/j.cattod.2005.10.021.
16) Joo, S. H.; Choi, S. J.; Oh, I.; Kwak, J.; Liu, Z.; Terasaki, O.; Ryoo, R., " Ordered nanoporous arrays of carbon supporting high dispersions of platinum nanoparticles," *Nature*, **412**, 169 (2001).doi: 10.1038/35084046.
17) Nam, J.-H.; Jang, Y.-Y.; Kwon, Y.-U.; Nam, J.-D., "Direct methanol fuel cell Pt-carbon catalysts by using SBA-15 nanoporous templates," *Electrochemistry Communications*, **6**, 737 (2004).doi: 10.1016/j.elecom.2004.05.016.
18) Antolini, E., "Graphene as a new carbon support for low-temperature fuel cell catalysts," *Applied Catalysis B: Environmental*, **123**, pp.52-68 (2012). doi:10.1016/j.apcatb.2012.04.022.
19) Antolini, E., "Carbon supports for low-temperature fuel cell catalysts," *Applied Catalysis B: Environmental*, **88**(1-2), 1-24 (2009). doi:10.1016/j.apcatb.2008.09.030.
20) Aranda, A., Murillo, R., Garcia, T., Callén, M.S. and Mastral, A.M., "Steam activation of tyre pyrolytic carbon black: Kinetic study in a thermobalance," *Chemical Engineering Journal*, **126(**2-3), 79-85 (2007). doi:10.1016/j.cej.2006.08.031.
21) Wibisono, Y., Amanah, A., Sukoyo, A., Anugroho, F. and Kurniati, E., "Activated Carbon Loaded Mixed Matrix Membranes Extracted from Oil Palm Empty Fruit Bunches for Vehicle Exhaust Gas Adsorbers," *Evergreen: joint journal of Novel Carbon Resource Sciences & Green Asia Strategy* **8**, Issue 03, 593-600 (2021). doi: 10.5109/4491651.
22) Abdullah, N.A., Rahardian, R., Hakim, I.I., Putra, N. and Koestoer, R.A., "Non-Sweep Gas Pyrolysis with Vap or Heater using "Shorea Pinanga" as a feedstock," *Evergreen: joint journal of Novel Carbon Resource Sciences & Green Asia Strategy* **7**(4), 555-563 (2020). doi: 10.5109/4150506.
23) Furutani, Y., Norinaga, K., Kudo, S., Hayashi, J.I. and Watanabe, T., "Current situation and future scope of biomass gasification in Japan," *Evergreen: joint journal of Novel Carbon Resource Sciences & Green Asia Strategy* **4**(24-29), 4 (2017). doi:10.5109/1929681.
24) Kotresh, K. M., & Belachew, M. G, "Study on waste tyre rubber as concrete aggregates," *International Journal of Scientific Engineering and Technology*, **3**(4), 433-436 (2014).
25) Thu, K., Miyazaki, T., Nakabayashi, K., Miyawaki, J. and Rahmawati, F., "Highly Microporous Activated Carbon from Acorn Nutshells and its Performance in Water Vapor Adsorption," *Evergreen: joint journal of Novel Carbon Resource Sciences & Green Asia Strategy* **8**, Issue 01, 249-254 (2021). doi: 10.5109/4372285.
26) Contescu, C. I., Adhikari, S. P., Gallego, N. C., Evans, N. D., & Biss, B. E. "Activated carbons derived from high-temperature pyrolysis of lignocellulosic biomass," *C*, **4**, 3, 51 (2018). doi:10.3390/c4030051
27) Chegini, G., Briens, C., & Pjontek, D. "Production and characterization of adsorbents from a hydrothermal char by pyrolysis, carbon dioxide and steam activation," *Biomass Conversion and Biorefinery*, 1-**17** (2022). doi:10.1007/s13399-022-02439-8
28) Erliyanti, N. K, Sangian, H. F., Susianto, S., Altway, A. "The Preparation Of Fixed Carbon Derived From Waste Tyre Using Pyrolysis," *Scientific Study & Research - Chemistry & Chemical Engineering, Biotechnology, Food Industry*, **16**, 4, (2016).
29) Taufany, F., Pan, C. J., Lai, F. J., Chou, H. L., Sarma, L. S., Rick, J., & Hwang, B. J., "Relating the composition of PtxRu100− x/C nanoparticles to their structural aspects and electrocatalytic activities in the methanol oxidation reaction," *Chemistry–A EuropeanJournal*, **19**(3), 905-915 (2013).doi: 10.1002/chem.201202473.
30) Merchant, A. A., & Petrich, M. A, "Pyrolysis of scrap tires and conversion of chars to activated carbon," *AIChE Journal*, **39**(8), 1370-1376 (1993).doi: 10.1002/aic.690390814.
31) Ridassepri, A.F., Rahmawati, F., Heliani, K.R., Miyawaki, J. and Wijayanta, A.T., "Activated carbon from bagasse and its application for water vapor adsorption," *Evergreen: joint journal of Novel CarbonResource Sciences & Green Asia Strategy* **7**, 409-416 (2020). doi: 10.5109/4068621.
32) Asnawi, T.M., Husin, H., Adisalamun, A., Rinaldi, W., Zaki, M. and Hasfita, F., "Activated carbons from palm kernels shells prepared by physical and chemical

activation for copper removal from aqueous solution," In *IOP Conference* Series: Materials Science And Engineering **543**(1), 012096. (2019).doi: 10.1088/1757-899X/543/1/012096.

33) Şahin, Ö., Saka, C., Ceyhan, A. A., & Baytar, O., "Preparation of high surface area activated carbon from Elaeagnus angustifolia seeds by chemical activation with $ZnCl_2$ in one-step treatment and its iodine adsorption," *Separation Science and Technology*, **50**(6), 886-891 (2015).doi: 10.1080/01496395.2014.966204.
34) Nayak, A., Bhushan, B., Gupta, V. and Sharma, P., "Chemically activated carbon from lignocellulosic wastes for heavy metal wastewater remediation: Effect of activation conditions," *Journal of colloid and interface science*, **493**, 228-240 (2017).doi: 10.1016/j.jcis.2017.01.031.
35) Zhang, H., Yan, Y. and Yang, L., "Preparation of activated carbon from sawdust by zinc chloride activation," *Adsorption*, **16**(3), 161-166 (2010).doi: 10.1007/s10450-010-9214-5.
36) Kusrini, E., Supramono, D., Muhammad, I.A., Pranata, S., Wilson, D.L. and Usman, A., "Effect of polypropylene plastic waste as co-feeding for production of pyrolysis oil from palm empty fruit bunches," *Evergreen: joint journal of Novel Carbon Resource Sciences & Green Asia Strategy* **6**(1), 92-97 (2019). doi:10.5109/2328410.
37) Zhou, J., Luo, A., & Zhao, Y., "Preparation and characterisation of activated carbon from waste tea by physical activation using steam," *Journal of the Air & Waste Management Association*, **68**(12), 1269-1277 (2018). doi: 10.1080/10962247.2018.1460282
38) Ahmad, M. A., Puad, N. A. A., & Bello, O. S, "Kinetic, equilibrium and thermodynamic studies of synthetic dye removal using pomegranate peel activated carbon prepared by microwave-induced KOH activation," *Water Resources and industry*, **6**, 18-35 (2014).doi: 10.1016/j.wri.2014.06.002.
39) Ukiwe, L. N., Oguzie, E., & Ajaero, C., "Adsorptive property, ash content analysis of activated carbon derived from three Nigerian Plants: Water hyacinth (Eichhornia crassipes), Iroko (Chloraphora excelsa), and Gmelina (Gmelina arborea)," *The African Journal of Plant Science and Biotechnology*, **2**(2), 109-111 (2008).doi:10.4314/ijonas.v3i3.36189.
40) Anisuzzaman, S. M., Joseph, C. G., Daud, W. M. A. B. W., Krishnaiah, D., & Yee, H. S.,"Preparation and characterization of activated carbon from Typha orientalis leaves," *International Journal of Industrial Chemistry*, **6**(1), 9-21 (2015).doi: 10.1007/s40090-014-0027-3.
41) Smisek, M and S. Cerny, "Active carbon: Manufacture, properties and application," *Elsevier Publishing Company*, New York (1970).doi: 10.1021/ac50160a026.
42) Sarma, L. S., Taufany, F., & Hwang, B. J., "*Electrocatalyst Characterization and Activity Validation–Fundamentals and Methods," Electrocatalysis of Direct Methanol Fuel Cells: From Fundamentals to Application*s, 115-163 (2009).doi: 10.1002/9783527627707.ch3.
43) Hwang, S. J., Yoo, S. J., Jeon, T. Y., Lee, K. S., Lim, T. H., Sung, Y. E., & Kim, S. K, "Facile synthesis of highly active and stable Pt–Ir/C electrocatalysts for oxygen reduction and liquid fuel oxidation reaction," *Chemical communications*, **46**(44), 8401-8403 (2010).doi: 10.1039/C0CC03125A.

Supporting Information

The Synthesis of Activated Carbon from Waste Tyre as Fuel Cell Catalyst Support

Fadlilatul Taufany[1*],Mathilda Jowito Pasaribu[1],Berlina Yunita Sari Romaji[1],Yeni Rah mawati[1],Ali Altway[1],Susianto[1],Siti Nurkhamidah[1],Julfikar Gilang Anfias[1], Yuliani Mursidah[1],Desi Fujanita[1],Susan Yulianti[1],Dian Rahmawati[1], Ghea Stellarosari[1]

[1]Department of Chemical Engineering, Institut Teknologi Sepuluh Nopember

*Author to whom correspondence should be addressed:
E-mail: f_taufany@chem-eng.its.ac.id

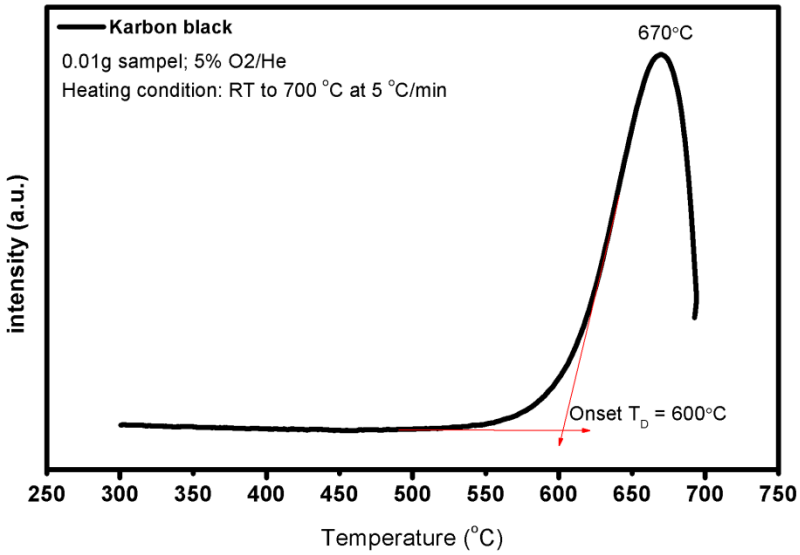

Figure S1: Temperature-programmed desorption (TPD) profile for the resulted pyrolytic carbon black.

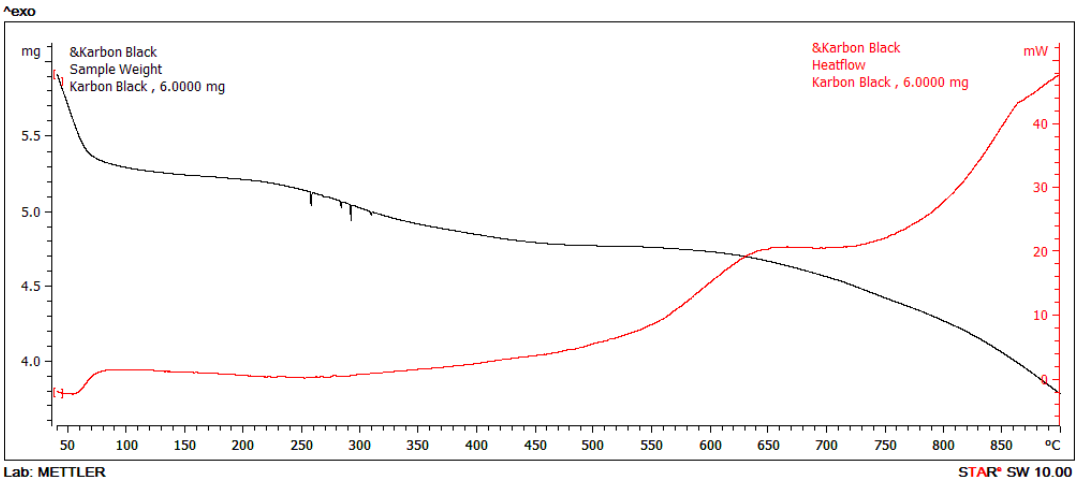

Figure S2: Mass loss profile of the resulted pyrolytic carbon black containing sample during thermogravimetric analysis (TGA).